JPET #113498

Base Excision Repair Proteins are Required for Integrin-Mediated Suppression of Bleomycin-Induced DNA Breakage in Murine Lung Endothelial Cells

Jane L. Rose[1], Kevin C. Reeves, Rostislav I. Likhotvorik, Dale G. Hoyt

Division of Pharmacology, The Ohio State University College of Pharmacy (J.L.R., K.C.R., R.I.L., D.G.H.), and The Dorothy M. Davis Heart and Lung Research Institute (D.G.H.), Columbus, OH 43210

1

JPET #113498

Running Title: BER proteins and integrin-mediated inhibition of DNA damage

Author for correspondence: Dale G. Hoyt, Ph.D.

Division of Pharmacology, The Ohio State University College of Pharmacy, 500 West

Twelfth Avenue, Columbus, OH, USA, 43210.

E-mail address: hoyt.27@osu.edu

Tel. (614) 292-6245; FAX (614) 292-9083

Text Pages: 27

Figures: 8

Tables: 0

Abstract: 226 words

Introduction: 626 words

Discussion: 1393 words

References: 40

Non-Standard Abbreviations:

Base Excision Repair, BER; Bleomycin, BLM; Deoxyribonuclease I, DNAse I; DNA-dependent protein kinase catalytic subunit, DNA-PK$_{CS}$; DNA ligase I, Lig1; DNA ligase III, Lig3; Dulbecco's minimum essential medium, DMEM; ethidium homodimer, ET2; ethylenediamine tetraacetic acid, EDTA; fetal bovine serum, FBS; green fluorescent protein, GFP; horseradish peroxidase, HRP; *In Situ* nick Translation ISNT; mouse lung endothelial cells, MLEC; non-homologous end joining, NHEJ; phosphate-buffered saline, PBS; poly(ADP-ribose) polymerase-1, PARP-1; polymerase chain reaction, PCR; small inhibitory RNA, siRNA; sodium dodecyl sulfate, SDS; X-ray repair complementing defective repair in Chinese hamster cells 1; XRCC1

Recommended section assignment:

Cellular and Molecular

Abstract

Engagement of integrin cell adhesion receptors suppresses bleomycin (BLM)-induced DNA strand breakage in endothelial cells. Previous investigation of cells from poly(ADP-ribose) polymerase-1 (PARP-1) knockout mice, and with an inhibitor of the enzyme, indicated that this facilitator of base excision repair (BER) is required for integrin-mediated suppression of DNA strand breakage. Here, small inhibitory RNA (siRNA) was used to assess the requirement for the BER proteins, DNA ligase III (Lig3) α, PARP-1, and XRCC1, and for the long-patch BER ligase, DNA ligase I (Lig1), in integrin-mediated protection from BLM-induced DNA breakage. Murine lung endothelial cells (MLEC) were transfected with siRNA, treated with anti-ß1 integrin antibody, and then BLM. 3'OH in DNA and accumulation of phosphorylated histone H2AX (γH2AX), which reflects double-strand breakage, were measured. Integrin antibody inhibited the increases in 3'OH caused by BLM in MLEC transfected with either control or Lig1 siRNA. However, after knockdown of Lig3α, PARP-1 or XRCC1, suppression of DNA breakage by integrin antibody was limited. BLM increased γH2AX levels, and integrin treatment inhibited this by 57 to 73% in MLEC transfected with control siRNA. Integrin engagement also inhibited increases in γH2AX in BLM-treated cells transfected with Lig1 siRNA. In contrast, Lig3α, PARP-1 and XRCC1 siRNAs prevented integrin-mediated inhibition of BLM-induced γH2AX levels. The results suggest that the BER proteins, Lig3α, PARP-1 and XRCC1, are required for integrin-mediated suppression of BLM-induced DNA breakage.

Introduction

Pharmacological manipulation of DNA damage may be important in the understanding,
medical application, and suppression of genotoxicity. Previously we found that engagement of
ß1 integrin cell adhesion receptors with antibodies inhibited acute, reversible DNA strand
breakage induced by bleomycin (BLM), bacterial endotoxin and etoposide in endothelial cells
(Hoyt et al., 1996; Hoyt et al., 1997; Jones et al., 2001; Huang et al., 2003). Integrins are a
family of heterodimeric cell surface proteins, composed of α and ß subunits that mediate
adhesion of cells to each other, the extracellular matrix and additional ligands. Integrin
engagement initiates intracellular signals that can promote endothelial cell survival, while a lack
of ligation or inappropriate engagement can induce apoptosis (Meredith et al., 1993; Stupack et
al., 2001; Juliano, 2002).

The ability of integrin engagement to inhibit DNA breakage caused by several unrelated
agents suggested that integrins act through mechanisms, such as altered nuclear architecture
or enhanced DNA repair, that could affect DNA breaks arising from diverse causes (Jones et al.,
2001; Huang et al., 2003; Rose et al., 2005). In fact, integrin-dependent protection of mouse
lung endothelial cell (MLEC) DNA was abolished in cells lacking the DNA repair facilitator,
poly(ADP-ribose) polymerase-1 (PARP-1), and in cells treated with a PARP-1 inhibitor (Jones et
al., 2001; Huang et al., 2003).

BLM is an anti-cancer antibiotic that cleaves DNA by iron-mediated activation of oxygen,
resulting in single- and double-strand DNA breaks (Chen and Stubbe, 2005). These breaks
require distinct pathways of repair. In Base Excision Repair (BER) of single-strand breaks,
PARP-1 is activated by 3'OH of broken DNA in a complex with XRCC1 and DNA ligase III (Lig3)
α (Masson et al., 1998; Caldecott, 2003; Fan and Wilson, 2005). In short patch BER, DNA
polymerase ß, interacting with X-ray repair complementing defective repair in Chinese hamster
cells 1 (XRCC1), replaces a single nucleotide and Lig3α seals the nicked DNA (Caldecott, 2003;
Dianova et al., 2004). Strand displacement replacing 2-12 bases can also occur in long patch
BER, with ligation mediated by Lig3α or DNA ligase I (Lig1) (Caldecott, 2003; Fan and Wilson,

2005). Lig3α is recruited to sites of damage in association with XRCC1, while a slower

recruitment of Lig1 depends on its association with proliferating cell nuclear antigen

(Mortusewicz et al., 2006). XRCC1 level and Lig3α activity regulate the degree of short vs. long

patch repair (Petermann et al., 2006).

The majority of double-strand DNA breaks are repaired by non-homologous end joining

(NHEJ) of DNA termini with final ligation by DNA ligase IV (Weterings and van Gent, 2004).

Upon double strand breakage the three phosphatidylinositol 3-kinase-like kinases, ataxia-

telangiectasia mutated (ATM), ataxia-telangiectasia mutated Rad3 related and DNA-dependent

protein kinase catalytic subunit (DNA-PK$_{CS}$) are activated and can phosphorylate the histone

variant, H2AX, at a conserved C-terminal SQ motif that is not present in H2A (Valerie and

Povirk, 2003). Immunocytochemical analysis demonstrated that phosphorylated H2AX, called

γH2AX, accumulates adjacent to double-strand breaks and facilitates recruitment of repair

proteins (Fernandez-Capetillo et al., 2004; Drouet et al., 2005). Interestingly, recent studies

indicate that BER proteins also play a role in repairing double-strand breaks (Audebert et al.,

2004; Wang et al., 2005; Audebert et al., 2006; Levy et al., 2006).

While integrin engagement suppresses 3'OH induced by several DNA damaging agents,

it is not known whether double-strand breakage is reduced. Furthermore, the sensitivity of

integrin-mediated suppression of DNA breakage to PARP-1 inhibition or deletion suggested that

PARP-1, or associated repair factors, may be required for integrin action. Given the role of BER

proteins in single- and double-strand repair, we investigated their role in integrin-mediated

protection of DNA. Specifically, we assessed the presence of DNA breaks by nick translation

labeling of 3'OH, and by immunofluorescence for γH2AX in integrin antibody- and BLM-treated

MLEC depleted of Lig1, Lig3α, XRCC1 or PARP-1.

Material and Methods

Endothelial cell growth supplement, heparin, phenylmethylsulfonyl fluoride, goat anti-rat IgG, phenol-chloroform-iso amyl alcohol, BLM and Bradford reagent were purchased from Sigma Chemical Co. (St Louis, MO). Fetal bovine serum was purchased from Hyclone Laboratories, Logan, UT. Rat anti-mouse ß1 integrin antibody was from PharMingen (San Diego, CA). DNA polymerase I was from New England Biolabs (Beverly, MA). Mouse monoclonal DNA ligase I antibody was from Novus Biologicals (Littleton, CO). Rabbit polyclonal XRCC1 antibody was purchased from Abcam (Cambridge, MA). Monoclonal PARP-1 antibody (Clone A6.4.12) was from Serotec (Raleigh, NC). Anti-phospho-histone H2A.X (Ser 139), Clone JBW301, was purchased from Upstate Biotechnologies Inc. (Charlottesville, VA). Cy3 and horseradish peroxidase (HRP)-conjugated goat anti-mouse and HRP-conjugated goat anti-rabbit secondary antibodies were from Jackson Immunoresearch Laboratories, Inc. (West Grove, PA). Renaissance Enhanced Chemiluminescence Reagent was purchased from New England Nuclear Life Sciences (Boston, MA). Bovine serum albumin, fluorescein-12-2'-deoxy-uridine-5'-triphosphate and anti-Lig3α antibody were obtained from Roche Applied Science (Indianapolis, IN). Silica chromatography filters were purchased from Quiagen (Valencia, CA). Dulbecco's minimum essential medium (DMEM), Trypsin, Trizol, Superscript Reverse Transcriptase, Platinum Taq DNA polymerase, Platinum PFX, pcDNA3.1 CT-GFP plasmid, RNAse-free DNAse, dCTP, dGTP, dATP nucleotides, ethidium homodimer (ET2) and H33342 were purchased from Invitrogen (Carlsbad, CA). Micron YM 100 molecular cutoff filters were from Millipore (Billerica, MA). Microspin G-25 columns were purchased from Amersham (Uppsala, Sweden). T7 RNA polymerase and ribonucleotides (RNA Maxx kit) were from Stratagene (La Jolla, CA). Recombinant Dicer was purchased from Ambion Corp. (Austin, TX). Tris-base, ethylenediamine tetraacetic acid (EDTA), NaCl, Na_3VO_4, NaF, Tween 20, formaldehyde, sodium dodecyl sulfate (SDS) and formaldehyde were from Fisher Scientific (Fair Lawn, NJ). Triton X-100 was purchased from Pierce (Rockford, IL). Female 129/Sv X C57Bl/6 mice were kindly

JPET #113498

donated by Dr. Csaba Szabó (Inotek Corporation, Beverly, MA; Current address: CellScreen

Applied Research Center, Semmelweis University Medical School, Budapest, Hungary).

siRNA

MLEC RNA was isolated by Trizol extraction. cDNA was synthesized using Superscript

Reverse Transcriptase. Amplification of the cDNA by polymerase chain reaction (PCR) was

then performed with pairs of 46 base primers containing a T7 RNA polymerase promoter

sequence (5'- GCG TAA TAC GAC TCA CTA TAG GGA GA) at the 5' end, followed by 20

bases of cDNA specific sequence. The cDNA specific sequences in Lig1, Lig3α, PARP-1, and

XRCC1 were designed from accession numbers NM010715, NM010716, BC012041, and

U02887, respectively. The following primer sets for PCR were therefore generated: Lig1, sense

5'-GCG TAA TAC GAC TCA CTA TAG GGA GAA AGC GAA GAA GCC AGA GAA G-3', anti-

sense 5'-GCG TAA TAC GAC TCA CTA TAG GGA GAG CGG TTG AGG CTG AGA TAG A-3';

Lig3α, sense 5'-GCG TAA TAC GAC TCA CTA TAG GGA GAC TGC CAT AAG TCA GTT CAG

C-3', anti-sense 5'-GCG TAA TAC GAC TCA CTA TAG GGA GAG ATC GTC TCT GAC ACG

TCA C-3'; PARP-1, sense 5'-GCG TAA TAC GAC TCA CTA TAG GGA GAT ATC GAG TGG

AGT ACG CGA A-3', anti-sense 5'-GCG TAA TAC GAC TCA CTA TAG GGA GAT TCA GGT

CGT TGG TGG AAC A-3'; XRCC1, sense 5'- GCG TAA TAC GAC TCA CTA TAG GGA GAC

AAG TAT CGG CCA GAC TGG A-3', anti-sense 5'- GCG TAA TAC GAC TCA CTA TAG GGA

GAA AGC GGT CAC GTA GCG GAT G-3'. Control siRNA was generated from a sequence

encoding a portion of green fluorescent protein (GFP) from plasmid pcDNA3.1 CT-GFP. A

primary template, lacking the plasmid's T7 promoter sequence, was first generated from the

plasmid by PCR using the sense primer 5'-GAG CTC GGA TCC ACT AGT C– 3', and anti-

sense primer 5'-GCA TGC CTG CTA TTG TCT– 3'. The primary PCR product was then used as

the template for PCR with the T7 promoter-containing primers, sense 5'-GCG TAA TAC GAC

TCA CTA TAG GGA GAA CTA CCT GTT CCA TGG CCA A-3' and anti-sense 5'-GCG TAA

TAC GAC TCA CTA TAG GGA GAA GCT CAT CCA TGC CAT GTG T-3'.

All PCR was carried out with high fidelity Platinum PFX polymerase. PCR products were verified for size by agarose electrophoresis and purified from PCR reactions by silica chromatography. The concentration of these transcription templates was determined from absorbance at 260 nm. The PCR products (0.4 μg), having a T7 promoter at each 5' end, were transcribed in vitro with T7 RNA polymerase (8 U/μl) and 4 mM of each ribonucleotide. The long double-stranded RNA was treated with RNAse-free DNAse, precipitated with ethanol, redissolved in water and measured by absorbance at 260 nm. One μg of long RNA was digested to approximately 21 bases by incubation for 18 h with 1 U recombinant Dicer in a 10 μl reaction containing 20 mM Tris pH 8, 150 mM NaCl and 2.5 mM $MgCl_2$. The small RNA was desalted with a Microspin G-25 column and purified by spin filtering with a Micron YM 100 molecular cutoff filter. SiRNA and its large precursor RNA were run in agarose gels and stained with ethidium bromide. Fluorescent digital images were recorded and quantified with image analysis software. The concentration of siRNA was calculated by comparison with the known amount of large RNA, assuming an average double-stranded RNA molecular weight of 13,629 g/mol.

Treatment of Cells

Endothelial cells were obtained from mouse lungs as described previously (Gerritsen et al., 1995; Jones et al., 2001; Huang et al., 2003; Rose et al., 2005). MLEC were cultured at 50% confluence in DMEM containing 20% FBS for 24 h. Cells were removed from flasks with trypsin, centrifuged (250 x g), washed once by resuspension and centrifugation in DMEM/20% FBS, and resuspended in 400 μl DMEM without serum. The cell suspension was incubated with 200 nM siRNA for 5 min, and placed in an aluminum-lined, 1 ml cuvette with a 0.4 cm gap, and electroporated with a single 20 ms pulse of 250 V at 975 μF using a Gene Pulser II electroporator (BioRad, Hercules, CA). MLEC were then cultured in DMEM/20% FBS for 24 h before protein extraction or further treatment. For integrin engagement, cells were treated with 0 or 1 μg anti-ß1 integrin antibody/ml for 1 h and then 2 μg goat anti-rat IgG for 4 h as previously

9

JPET #113498

described (Hoyt et al., 1996; Hoyt et al., 1997; Jones et al., 2001; Huang et al., 2003; Rose et

al., 2005). Medium or BLM was then added for 15 or 45 min.

Western Blotting

MLEC were washed 3 times with ice-cold PBS and lysed with lysis buffer containing 1% triton X-

100, 50 mM Tris pH 7.5, 150 mM NaCl, 5 mM EDTA, 0.5 mM Na_3VO_4, 50 mM NaF, 10 µg/ml

aprotinin, 10 µg/ml leupeptin, 10 µg/ml pepstatin A and 1 mM phenylmethylsulfonyl fluoride.

Extracts were sonicated and protein concentration was determined by the Bradford assay as

described previously (Rose et al., 2005). Ten µg of protein was incubated with protein loading

buffer and incubated for 10 min at 95°C. Proteins were separated on 4-20% Tris-gylcine

polyacrylamide gels and transferred to nitrocellulose.

After transfer, the blots were blocked with 3% non-fat dry milk in Tris-buffered saline buffer and

Tween 20 (0.1%Tween 20, 10 mM Tris, pH 7.5 and 150 mM NaCl) and probed with primary

antibody for 1 h at room temperature. After blots were washed, appropriate HRP-conjugated

secondary antibody was added and incubated for 1 h. Proteins were visualized using enhanced

chemiluminescent reagents and captured on X-ray film. Films were scanned to produce digital

images for analysis.

In Situ Nick Translation (ISNT)

Relative levels of 3'OH in DNA were labeled by ISNT with a fluorescent nucleotide as described

previously (Gorczyca et al., 1993; Hoyt et al., 1997; Jones et al., 2001; Huang et al., 2003).

After treatments, cells were fixed with 1% formaldehyde for 10 min at 37°C. Cells were washed

three times with PBS and made permeable by incubation overnight in 70% ethanol at -20°C.

Cells were washed three times with PBS at 4°C and then incubated at 37°C for 90 min with

ISNT buffer (2.5 mM $MgCl_2$, 50 mM Tris pH 7.8, 10 mM ß-mercaptoethanol and 10 µg/ml bovine

serum albumin) containing 16 µM each dGTP, dATP and dCTP, fluorescein-12-2'-deoxy-

10

uridine-5'- triphosphate, and 2 U/ml *E. coli* DNA polymerase. Labeling was stopped by rinsing

with PBS. An Olympus BX60 fluorescence microscope and 20X objective were used to image

fluorescein (blue excitation/green emission) and to record digital microscopic images.

Immunofluorescence for γH2AX

After treatments, MLEC were fixed in 95% ethanol/ 5% acetic acid for 5 min at 4°C and rinsed 3

times with Tris-buffered saline (10 mM Tris, pH 7.5 and 150 mM NaCl). MLEC were blocked

with 10% goat serum in Tris-buffered saline for 1 h, probed with a 1:500 dilution of anti-γH2AX

antibody in 10% goat serum/Tris-buffered saline for 1 h and a 1:400 dilution of goat anti-mouse

conjugated Cy3 secondary antibody in 10% goat serum/Tris-buffered saline for 1.5 h. Digital

microscopic images of Cy3-labeled nuclei (green excitation/red emission) were recorded as for

ISNT.

Cytotoxicity

Cytotoxicity of BLM was assessed, as described previously (Huang et al., 2003), by cell

permeability to ET2, which fluoresces when bound to DNA after entering cells. MLEC were

electroporated with GFP or XRCC1 siRNA, cultured for 24 h, incubated with antibodies, and

treated with 0-500 µg BLM/ml for 4 h. Cells were washed and incubated 20 min in medium

containing 4 µM ET2 and 310 µM H33342, a cell-permeable bisbenzamide DNA stain. UV

excitation and blue emission for H33342 was used to objectively identify nuclei in microscopic

fields, and digital images of ET2 (green excitation/red emission) were recorded.

Data Analysis

Protein levels in western blots and average intensity of nuclei in microscopic images were

determined with image analysis software (Scanpro, SPSS Science, Chicago, IL) as described

previously (Hoyt et al., 1997; Jones et al., 2001; Huang et al., 2003; Rose et al., 2005). Data

were analyzed by Student's *t* test or by analysis of variance (ANOVA) with Bonferroni correction

for multiple comparisons (Snedecor and Cochran, 1980).

Results

Figure 1 demonstrates the depletion of Lig1, PARP-1, Lig3α and XRCC1 protein 24 h after

transfection of MLEC with siRNAs. Lig1 protein was reduced to 7% of GFP control siRNA levels

in Lig1 siRNA transfected MLEC (figure 1a). Lig3α siRNA depleted Lig3α protein to 34% of

control levels (figure 1b). PARP-1 siRNA preferentially depleted PARP-1 protein to 20% of

control levels (figure 1c), while XRCC1 siRNA reduced XRCC1 protein to 34% of control siRNA

(figure 1d). XRCC1 siRNA also reduced the levels of Lig3α (figure 1b). This result is consistent

with the ability of XRCC1 protein to stabilize Lig3α protein through their physical interaction

(Caldecott et al., 1994), and was observed with a different XRCC1 siRNA in another cell type

(Petermann et al., 2006).

The effect of knockdown of Lig1 and Lig3α on BLM-induced DNA strand breakage was

assessed. In MLEC transfected with the control siRNA, 0.2, 0.5 and 1.0 mg BLM/ml

significantly increased DNA strand breakage measured by ISNT of 3'OH, and reductions in

3'OH after a 1 h drug-free recovery period were observed (figure 2a). In cells transfected with

either Lig1 or Lig3α siRNAs the removal of 3'OH was antagonized (figure 2b-c), confirming the

activity of these siRNAs. Anti-ß1 integrin antibody suppressed 3'OH induced by 0.2, 0.5 and 1.0

BLM by 71, 48 and 66%, respectively, in cells transfected with control siRNA (figure 3a).

Integrin-meditated protection was also observed with Lig1 siRNA, where 3'OH labeling in cells

treated with 0.2, 0.5 and 1.0 BLM cells was reduced, respectively, by 61, 66, and 58% (figure

3b). However, no inhibition of BLM-induced DNA breakage by the integrin antibody was seen in

cells transfected with Lig3α siRNA (figure 3c). In MLEC treated with anti-ß1 integrin antibody

and 0.5 mg BLM/ml, and allowed a washout period (figure 3a-c, right side of panels), 3'OH

labeling was not different from the level in antibody-treated cells before washout. In particular,

3'OH remained elevated following washout in cells treated with Lig3α siRNA, treated with anti-ß1 integrin antibody (figure 3c).

Knockdown of XRCC1 increased the 3'OH labeling caused by 0.2, 0.5 and 1.0 mg BLM/ml in comparison with control siRNA-treated cells (figure 4, open bars). With control siRNA, elevated 3'OH labeling was reduced to insignificant levels after 1 h incubation in BLM-free medium (figure 4a, washout, single hatched bars). Each group of XRCC1 siRNA-treated cells (figure 4b) exhibited increased 3'OH labeling in comparison with the same group treated with control siRNA (p<0.05 for each comparison of groups in figure 4b with 4a). Thus, XRCC1 siRNA increased the level of breakage during incubation with BLM, and after a 1 h washout with or without integrin engagement. ß1 integrin antibody suppressed DNA breaks caused by 0.5-1.0 mg BLM/ml in control siRNA-transfected cells (figure 4a). With 1.0 mg BLM/ml, the reduction was by 94%, for example. However, in cells transfected XRCC1 siRNA, 3'OH labeling induced by 0.2-1.0 mg BLM/ml was partially reduced by ß1 integrin antibody, but was still significant (figure 4b, solid bars). Here the reduction by integrin engagement was 51% in XRCC1 siRNA-transfected cells treated with 1.0 mg BLM/ml. Recovery after washout was inhibited by XRCC1 siRNA: although 3'OH labeling decreased after washout of 0.5 and 1.0 mg BLM/ml by 66 and 75% of the unwashed groups, respectively, in control siRNA-treated cells, the decreases were only by 9 and 34% with XRCC1 siRNA. Furthermore, while recovery was complete after 0.2 mg BLM/ml in XRCC1 siRNA plus ß1 integrin antibody-treated cells, it was completely blocked in those MLEC treated with 0.5 or 1.0 mg BLM/ml. Integrin-mediated inhibition of DNA strand breaks was also prevented by PARP-1 siRNA in comparison with control siRNA in another independent experiment (figure 5).

γH2AX, or H2AX phosphorylated at S^{139} in its C-terminal domain, is an indirect indicator of double-strand DNA breaks in cells exposed to genotoxic agents (Valerie and Povirk, 2003). A specific antibody revealed the concentration-dependent effect of BLM on H2AX phosphorylation figure 6. Image analysis indicated that exposure to BLM for 15 min significantly increased the level of γH2AX in MLEC (figure 6b).

13

Based on these results, MLEC were transfected with siRNA, treated with integrin antibody, and then challenged with BLM for 15 min. As expected, in the absence of integrin engagement BLM increased γH2AX levels in cells transfected with control siRNA (figure 7a). Pretreatment with anti-ß1 integrin antibody reduced γH2AX fluorescence intensity by 73% in MLEC treated with 25 µg BLM/ml and 57% in cells exposed to 100 µg BLM/ml (figure 7a). In Lig1 siRNA-transfected MLEC, integrin antibody also reduced γH2AX immunofluorescence by 58 and 44% after treatment with 25 and 100 µg BLM/ml respectively (figure 7b). However, depletion of Lig3α, PARP-1 or XRCC1 severely compromised this integrin-mediated inhibition (figures 7c-e). In the case of XRCC1 siRNA, the induction of γH2AX by BLM was actually enhanced by treatment with anti-ß1 integrin-antibody.

Given the differing effect of XRCC1 siRNA on integrin modulation of 3'OH and γH2AX, the effect of this siRNA on acute cytotoxicity of 100 and 500 µg BLM/ml BLM was measured. BLM caused a concentration-dependent increase in permeability to ET2 in MLEC electroporated with control siRNA and engagement of ß1 integrins prevented it (figure 8e). XRCC1 siRNA alone reduced the permeability caused by 100 µg BLM /ml, and integrin engagement did not further reduce it (figure 8f). While the increased permeability caused by 500 µg BLM/ml was not affected by XRCC1 siRNA, integrin-mediated protection from this concentration was partially inhibited (figure 8f).

Discussion

BLM is a useful anticancer agent that has a relatively low potential for myelosuppressive side effects. It can however cause lung disease, in part as a consequence of damage to pulmonary endothelial cells (Hoyt et al., 1997). Suppression of acute DNA damage in normal tissue might be a beneficial clinical adjunct. More generally, stimulation or inhibition of DNA damage via cell surface receptors may be particularly useful.

Engagement of ß1 integrin receptors was found to inhibit endotoxin-, etoposide- and BLM-induced DNA strand breakage as measured by 3'OH labeling (Hoyt et al., 1996; Jones et

14

al., 2001; Huang et al., 2003). Investigation with a PARP-1 inhibitor and in PARP-1 knockout

MLEC indicated that integrin-dependent reduction in 3'OH breaks requires the BER facilitator,

PARP-1 (Jones et al., 2001; Huang et al., 2003). Roles for other single-strand repair proteins in

integrin action had not been examined. SiRNA techniques allow such investigations where

useful antagonists or knockouts are unavailable.

Knockdown of Lig1 and Lig3α both antagonized the removal of 3'OH during a 1 h drug-

free recovery phase (figure 2). This inhibition of recovery is consistent with roles for both ligases

in DNA repair (Leppard et al., 2003; Mortusewicz et al., 2006). Lig3α, but not Lig1, siRNA

antagonized the ability of integrin engagement to suppress BLM-induced DNA breakage (figure

3). In addition, with integrin engagement 3'OH remained low after 1 h washout in Lig1 siRNA-

treated cells (figure 3b), but remained elevated with Lig3α siRNA (figure 3c). These results

suggest that integrin action depends selectively on the short patch BER ligase component, and

not all DNA ligases.

Knockdown of XRCC1 increased the level of 3'OH DNA breaks caused by BLM (figure

4a). This result is similar to that of another XRCC1 siRNA on alkylating agent-induced DNA

breakage in HeLa cells (Petermann et al., 2006) and presumably reflects a critical role of this

protein in DNA repair. Integrin-mediated suppression of 3'OH DNA breaks was partially

antagonized by XRCC1 siRNA, and 3'OH were still elevated 1 h after BLM-free washout with or

without integrin engagement (figure 4). Since XRCC1 siRNA also reduced Lig3α levels (figure

1b) (Petermann et al., 2006), it was expected that integrin action would be extensively blocked

as seen with Lig3α siRNA (figure 3c). Other evidence suggests that long patch repair with

ligation of DNA 3'OH by Lig1 is facilitated when XRCC1 and Lig3α are deficient (Caldecott,

2003; Fan and Wilson, 2005; Petermann et al., 2006). Thus, we speculate that antagonism of

integrin-mediated suppression of 3'OH DNA breaks by XRCC1 siRNA might be limited to some

extent by alternative repair mechanisms that become operational. In any case, BLM-induced

DNA breakage and its inhibition by integrin engagement were sensitive to XRCC1 knockdown.

As expected, siRNA knockdown of PARP-1 inhibited integrin action, confirming the prior indications that PARP-1 is required for integrin-mediated protection (figure 5) (Jones et al., 2001; Huang et al., 2003). Although PARP-1 does not modify damaged DNA during repair, it binds to 3'OH and is allosterically activated to modify several repair proteins and histones with polymers of ADP-ribose. The potential for these polymers to stimulate ligation, and the association of PARP-1 with XRCC1 and Lig3α are consistent with the requirement for PARP-1 in integrin action (Masson et al., 1998; Oei and Ziegler, 2000; Caldecott, 2003; Leppard et al., 2003; Fan and Wilson, 2005). Overall, the results indicate that integrin-mediated suppression of BLM-induced 3'OH DNA breaks depends on PARP-1, XRCC1 and Lig3α, which are physically interacting BER components with a recognized role in short patch repair of single-strand breaks (Masson et al., 1998; Caldecott, 2003; Fan and Wilson, 2005).

BLM can also generate double-strand breaks and activate ATM (Chen and Stubbe, 2005; Fernandes et al., 2005). Radiation-induced double-strand breaks were originally correlated with phosphorylation of histone variant H2AX (Rogakou et al., 1998). Subsequent studies with γH2AX-specific antibodies correlated staining with double-strand DNA breaks assessed by other methods (Paull et al., 2000; Nazarov et al., 2003). As in other cell types (Banath and Olive, 2003), BLM caused a concentration-dependent increase in γH2AX in MLEC here (figure 6).

While suppression of drug-induced DNA 3'OH strand breaks by integrin engagement has been repeatedly seen (figures 3-5) (Hoyt et al., 1996; Hoyt et al., 1997; Jones et al., 2001; Huang et al., 2003), we found here for the first time that integrin engagement suppressed the induction of γH2AX by BLM (figure 7). Lig3α, PARP-1 or XRCC1, but not Lig1, siRNA antagonized integrin-mediated reductions. Integrin-mediated suppression of 3'OH and acute cytotoxicity were each partially inhibited by XRCC1 siRNA (figures 4 and 8), suggesting a correlation between these two endpoints. Interestingly, the γH2AX response to 100 μg BLM/ml was actually increased by integrin engagement after treatment with XRCC1 siRNA (figure 7d), while cytotoxicity was not (figure 8f). As discussed below, XRCC1 appears to function in both

BER and NHEJ pathways. It is possible that BER and NHEJ may require different levels of XRCC1 or Lig3α for normal function and for the response to integrin engagement. Complete depletion or knockout of XRCC1 or Lig3α might also have different effects than the partial knockdowns attained with siRNA. Given that XRCC1 siRNA reduced both XRCC1 and Lig3α, while Lig3α siRNA selectively depleted Lig3α, we would hypothesize that depletion of XRCC1 permits integrin engagement to facilitate increases in γH2AX in response to BLM. Since the level of γH2AX is actually a balance between kinase and phosphatase activities acting on this histone (Nazarov et al., 2003), H2AX kinases or phosphatases could be modulated by integrin engagement in a manner that is dependent on XRCC1. Nevertheless, the results suggest that PARP-1, XRCC1 and Lig3α, but not Lig1, are required for integrin-mediated suppression of BLM-induced double-strand breakage.

The involvement of PARP-1, XRCC1 and Lig3α in the suppression of double-strand breakage by integrin engagement might be due to possible effects of these BER components on conversion of isolated single strand breaks, or clusters of them, to double strand breaks. Recent investigations also indicate that PARP-1, XRCC1 and Lig3α contribute to repair of double-strand breaks in vitro, and to cellular resistance to double-strand breaking agents (Audebert et al., 2004; Audebert et al., 2006). In addition, ionizing radiation induced DNA-PK$_{CS}$ to phosphorylate XRCC1, and γH2AX accumulation was increased by expression of a non-phosphorylatable mutant of XRCC1 in comparison with wildtype (Levy et al., 2006). Lig3 also associated with the NHEJ proteins, Ku70 and 80, as indicated by their retention on a Lig3 affinity column (Leppard et al., 2003), and DNA ligase IV deficient cells retained a substantial level of DNA end-joining activity which was reduced 80% by a Lig3α siRNA (Wang et al., 2005). Finally, EM9 and EM-C11 cell lines lacking XRCC1 displayed slower repair of double-strand breaks compared to cells containing XRCC1 (Schwartz et al., 1987; Nocentini, 1999). Thus, multiple functions of BER proteins in single- and double-strand DNA repair may account for their requirement in integrin-mediated suppression of DNA 3'OH and γH2AX levels in BLM-treated MLEC.

17

Integrin engagement may increase PARP-1/XRCC1/Lig3α-dependent repair of single- and double-strand breaks. Mechanisms that could be responsible for this potential effect are not known, but integrin engagement could modify the repair proteins or the DNA substrate. For example, chromatin structural proteins may be altered so that repair is more efficient. Growing evidence implicates chromatin modifications in the repair of strand breaks (Bird et al., 2002; Peterson and Cote, 2004; Verger and Crossley, 2004). Efficient repair of double-strand breaks through NHEJ requires stabilization of the ends of DNA by Ku70/80 proteins and DNA-PK$_{CS}$ (Weterings and van Gent, 2004; Wang et al., 2005), and this step may be facilitated by chromatin structural proteins (Iliakis et al., 2004). Previously we found that integrin engagement increased the sensitivity of MLEC DNA to nuclease digestion, increased the acetylation of histone 3, and generally reduced the association of linker histone 1 with DNA (Jones et al., 2001; Rose et al., 2005). Thus, integrin-mediated effects on chromatin structure may make DNA breaks more manageable by PARP-1/XRCC1/Lig3α in the repair process. Alternatively, integrin engagement may increase BER protein activities that enhance repair of single- and/or double-strand breaks.

In summary, integrin engagement reduced both 3'OH and γH2AX caused by BLM in MLEC. Protection was antagonized by suppression of the BER proteins, PARP-1, XRCC1 and Lig3α, but not Lig1. These results suggest potential targets for pharmacological intervention in genotoxicity through BER proteins, and indicate a novel mechanism by which integrin engagement protects endothelial cells from DNA damage.

JPET #113498

References

Audebert M, Salles B and Calsou P (2004) Involvement of PARP-1 and XRCC1/DNA ligase III in an alternative route for DNA double-strand breaks rejoining. *J Biol Chem* **279**:55117-55126.

Audebert M, Salles B, Weinfeld M and Calsou P (2006) Involvement of polynucleotide kinase in a poly(ADP-ribose) polymerase-1-dependent DNA double-strand breaks rejoining pathway. *J Mol Biol* **356**:257-265.

Banath JP and Olive PL (2003) Expression of phosphorylated histone H2AX as a surrogate of cell killing by drugs that create DNA double-strand breaks. *Cancer Res* **63**:4347-4350.

Bird AW, Yu DY, Pray-Grant MG, Qiu Q, Harmon KE, Megee PC, Grant PA, Smith MM and Christman MF (2002) Acetylation of histone H4 by Esa1 is required for DNA double-strand break repair. *Nature* **419**:411-415.

Caldecott KW (2003) XRCC1 and DNA strand break repair. *DNA Repair (Amst)* **2**:955-969.

Caldecott KW, McKeown CK, Tucker JD, Ljungquist S and Thompson LH (1994) An interaction between the mammalian DNA repair protein XRCC1 and DNA ligase III. *Mol Cell Biol* **14**:68-76.

Chen J and Stubbe J (2005) Bleomycins: towards better therapeutics. *Nat Rev Cancer* **5**:102-112.

Dianova, II, Sleeth KM, Allinson SL, Parsons JL, Breslin C, Caldecott KW and Dianov GL (2004) XRCC1-DNA polymerase beta interaction is required for efficient base excision repair. *Nucleic Acids Res* **32**:2550-2555.

Drouet J, Delteil C, Lefrancois J, Concannon P, Salles B and Calsou P (2005) DNA-dependent protein kinase and XRCC4-DNA ligase IV mobilization in the cell in response to DNA double strand breaks. *J Biol Chem* **280**:7060-7069.

Fan J and Wilson DM, 3rd (2005) Protein-protein interactions and posttranslational modifications in mammalian base excision repair. *Free Radic Biol Med* **38**:1121-1138.

JPET #113498

Fernandes N, Sun Y, Chen S, Paul P, Shaw RJ, Cantley LC and Price BD (2005) DNA damage-induced association of ATM with its target proteins requires a protein interaction domain in the N terminus of ATM. *J Biol Chem* **280**:15158-15164.

Fernandez-Capetillo O, Lee A, Nussenzweig M and Nussenzweig A (2004) H2AX: the histone guardian of the genome. *DNA Repair (Amst)* **3**:959-967.

Gerritsen ME, Shen CP, McHugh MC, Atkinson WJ, Kiely JM, Milstone DS, Luscinskas FW and Gimbrone MA, Jr. (1995) Activation-dependent isolation and culture of murine pulmonary microvascular endothelium. *Microcirculation* **2**:151-163.

Gorczyca W, Gong J and Darzynkiewicz Z (1993) Detection of DNA strand breaks in individual apoptotic cells by the in situ terminal deoxynucleotidyl transferase and nick translation assays. *Cancer Res* **53**:1945-1951.

Hoyt DG, Rizzo M, Gerritsen ME, Pitt BR and Lazo JS (1997) Integrin activation protects pulmonary endothelial cells from the genotoxic effects of bleomycin. *Am J Physiol* **273**:L612-617.

Hoyt DG, Rusnak JM, Mannix RJ, Modzelewski RA, Johnson CS and Lazo JS (1996) Integrin activation suppresses etoposide-induced DNA strand breakage in cultured murine tumor-derived endothelial cells. *Cancer Res* **56**:4146-4149.

Huang H, McIntosh JL, Fang L, Szabo C and Hoyt DG (2003) Integrin-mediated suppression of endotoxin-induced DNA damage in lung endothelial cells is sensitive to poly(ADP-ribose) polymerase-1 gene deletion. *Int J Mol Med* **12**:533-540.

Iliakis G, Wang H, Perrault AR, Boecker W, Rosidi B, Windhofer F, Wu W, Guan J, Terzoudi G and Pantelias G (2004) Mechanisms of DNA double strand break repair and chromosome aberration formation. *Cytogenet Genome Res* **104**:14-20.

Jones CB, McIntosh J, Huang H, Graytock A and Hoyt DG (2001) Regulation of bleomycin-induced DNA breakage and chromatin structure in lung endothelial cells by integrins and poly(ADP-ribose) polymerase. *Mol Pharmacol* **59**:69-75.

Juliano RL (2002) Signal transduction by cell adhesion receptors and the cytoskeleton:

functions of integrins, cadherins, selectins, and immunoglobulin-superfamily members.

Annu Rev Pharmacol Toxicol **42**:283-323.

Leppard JB, Dong Z, Mackey ZB and Tomkinson AE (2003) Physical and functional interaction

between DNA ligase IIIalpha and poly(ADP-Ribose) polymerase 1 in DNA single-strand

break repair. *Mol Cell Biol* **23**:5919-5927.

Levy N, Martz A, Bresson A, Spenlehauer C, de Murcia G and Menissier-de Murcia J (2006)

XRCC1 is phosphorylated by DNA-dependent protein kinase in response to DNA

damage. *Nucleic Acids Res* **34**:32-41.

Masson M, Niedergang C, Schreiber V, Muller S, Menissier-de Murcia J and de Murcia G (1998)

XRCC1 is specifically associated with poly(ADP-ribose) polymerase and negatively

regulates its activity following DNA damage. *Mol Cell Biol* **18**:3563-3571.

Meredith JE, Jr., Fazeli B and Schwartz MA (1993) The extracellular matrix as a cell survival

factor. *Mol Biol Cell* **4**:953-961.

Mortusewicz O, Rothbauer U, Cardoso MC and Leonhardt H (2006) Differential recruitment of

DNA Ligase I and III to DNA repair sites. *Nucleic Acids Res* **34**:3523-3532.

Nazarov IB, Smirnova AN, Krutilina RI, Svetlova MP, Solovjeva LV, Nikiforov AA, Oei SL,

Zalenskaya IA, Yau PM, Bradbury EM and Tomilin NV (2003) Dephosphorylation of

histone gamma-H2AX during repair of DNA double-strand breaks in mammalian cells

and its inhibition by calyculin A. *Radiat Res* **160**:309-317.

Nocentini S (1999) Rejoining kinetics of DNA single- and double-strand breaks in normal and

DNA ligase-deficient cells after exposure to ultraviolet C and gamma radiation: an

evaluation of ligating activities involved in different DNA repair processes. *Radiat Res*

151:423-432.

Oei SL and Ziegler M (2000) ATP for the DNA ligation step in base excision repair is generated

from poly(ADP-ribose). *J Biol Chem* **275**:23234-23239.

Paull TT, Rogakou EP, Yamazaki V, Kirchgessner CU, Gellert M and Bonner WM (2000) A
critical role for histone H2AX in recruitment of repair factors to nuclear foci after DNA
damage. *Curr Biol* **10**:886-895.

Petermann E, Keil C and Oei SL (2006) Roles of DNA ligase III and XRCC1 in regulating the
switch between short patch and long patch BER. *DNA Repair (Amst)* **5**:544-555.

Peterson CL and Cote J (2004) Cellular machineries for chromosomal DNA repair. *Genes Dev*
18:602-616.

Rogakou EP, Pilch DR, Orr AH, Ivanova VS and Bonner WM (1998) DNA double-stranded
breaks induce histone H2AX phosphorylation on serine 139. *J Biol Chem* **273**:5858-
5868.

Rose J, Huang H, Wray S and Hoyt D (2005) Integrin engagement increases histone H3
acetylation and reduces histone H1 association with DNA in murine lung endothelial
cells. *Mol Pharmacol* **68**:439-446.

Schwartz JL, Giovanazzi S and Weichselbaum RR (1987) Recovery from sublethal and
potentially lethal damage in an X-ray-sensitive CHO cell. *Radiat Res* **111**:58-67.

Snedecor G and Cochran W (1980) *Statistical Methods*. Iowa State University Press, Ames.

Stupack DG, Puente XS, Boutsaboualoy S, Storgard CM and Cheresh DA (2001) Apoptosis of
adherent cells by recruitment of caspase-8 to unligated integrins. *J Cell Biol* **155**:459-
470.

Valerie K and Povirk LF (2003) Regulation and mechanisms of mammalian double-strand break
repair. *Oncogene* **22**:5792-5812.

Verger A and Crossley M (2004) Chromatin modifiers in transcription and DNA repair. *Cell Mol
Life Sci* **61**:2154-2162.

Wang H, Rosidi B, Perrault R, Wang M, Zhang L, Windhofer F and Iliakis G (2005) DNA ligase
III as a candidate component of backup pathways of nonhomologous end joining.
Cancer Res **65**:4020-4030.

Weterings E and van Gent DC (2004) The mechanism of non-homologous end-joining: a

synopsis of synapsis. *DNA Repair (Amst)* **3**:1425-1435.

JPET #113498

Footnotes

a) Unnumbered Footnote:

This work was supported by HL68054 from the National Heart, Lung, and Blood Institute. Its

contents are solely the responsibility of the authors and do not necessarily represent the official

views of the National Heart, Lung, and Blood Institute or NIH.

b) Person to receive reprint requests

Dale G. Hoyt, PhD

Division of Pharmacology

The Ohio State University College of Pharmacy

500 West Twelfth Avenue

Columbus, OH, USA, 43210

E-mail address: hoyt.27@osu.edu

c) Numbered Footnote

[1]*Current address*: Department of Medicine, Division of Pulmonary, Allergy, and Critical Care

Medicine, University of Pittsburgh School of Medicine, 3459 Fifth Ave, NW 640 MUH ,

Pittsburgh, Pennsylvania 15213, USA.

Legends for Figures

Figure 1. Effect of siRNA on Lig1, PARP-1, Lig3α and XRCC1 protein levels. MLEC were transfected with 200 nM GFP (Open bars), XRCC1 (Solid bars), Lig3α (Checked bars), PARP-1 (Vertical striped bar), or Lig1 (Diagonal striped bars) siRNA and protein was extracted after 24 h. Images are representative western blots for Lig1 (**A**), Lig3α (**B**) PARP-1 (**C**) or XRCC1 (**D**) proteins. Bars represent mean + S.E. of densitometric analysis of western blots of 3 independent transfections of each siRNA. *, p <0.05 for comparison with GFP siRNA.

Figure 2. Effects of knockdown of Lig1 and Lig3α and drug washout on BLM-induced DNA strand breakage measured by ISNT. MLEC were transfected as in figure 1 with GFP (**A**), Lig1 (**B**) or Lig3α (**C**) siRNA. Twenty four h later cells were treated with 0, 0.2, 0.5, or 1.0 mg BLM/ml for 45 min, and incubated for 0 ("Treatment") or 1 h ("Washout") in BLM-free medium processed for measurement of 3'OH DNA strand breaks by ISNT. Bars represent the mean difference in nuclear fluorescence intensity between BLM- and vehicle-treated cells + SE for 100-200 cells in each experimental group. *, p <0.05 for comparison with 0 mg BLM/ml (or a mean difference of 0 on the vertical axis). +, p<0.05 for comparison of 0 and 1 h washout.

Figure 3. Effects of knockdown of Lig1 and Lig3α integrin-mediated suppression of BLM-induced DNA strand breakage measured by ISNT. MLEC were transfected as in figure 2. Twenty four h later cells were treated with 0 or 1 µg anti-ß1 integrin antibody/ml for 1 h and then with goat-anti rat IgG (2 µg/ml final concentration) for 4 h. Cells were then treated with 0, 0.2, 0.5 or 1.0 mg BLM/ml for 45 min and incubated for incubated for 0 ("Treatment") or 1 h in BLM-free medium ("Washout", after 0.5 mg BLM/ml), and processed for measurement of 3'OH DNA strand breaks by ISNT. Bars represent the mean difference in nuclear fluorescence intensity between BLM- and vehicle-treated cells + SE for 100-200 cells in each experimental group. *, p <0.05 for comparison with 0 mg BLM/ml (or a mean difference of 0 on the vertical axis). +, p<0.05 for comparison with no anti-ß1 integrin antibody for each BLM concentration. #, p <0.05 for comparison of the similarly treated washout and no washout ("Treatment") groups.

Figure 4. Effects of knockdown of XRCC1 and drug washout on integrin-mediated suppression of BLM-induced DNA strand breakage measured by ISNT. MLEC were transfected with 200 nM GFP (**A**) or XRCC1 siRNA (**B**). Twenty four h later ß1 integrins were engaged as in figure 3. Cells were then treated with 0-1 mg BLM/ml for 45 min and incubated for incubated for 0 ("Treatment") or 1 h in BLM-free medium ("Washout"), and processed for measurement of 3'OH DNA strand breaks by ISNT. Bars represent the mean difference in nuclear fluorescence intensity between BLM- and vehicle-treated cells + SE for 400-2000 cells

in each experimental group. *, $p < 0.05$ for comparison with 0 mg BLM/ml (or a mean difference of 0 on the vertical axis). +, p<0.05 for comparison with no anti-ß1 integrin antibody. #, $p < 0.05$ for comparison with no washout ("Treatment") group treated in the same manner. All groups in panel B were significantly elevated in comparison with the same group in panel A ($p < 0.05$).

Figure 5. Effects of knockdown of PARP-1 on integrin-mediated suppression of BLM-induced DNA strand breakage measured by ISNT. MLEC were transfected with 200 nM GFP or PARP-1 siRNA. Twenty four h later ß1 integrins were engaged as in figure 3. Cells were then treated with 0 or 1 mg BLM/ml for 45 min and processed for ISNT. Bars represent the mean difference in nuclear fluorescence intensity between BLM- and vehicle-treated cells + SE for 400-2000 cells in each experimental group. *, $p < 0.05$ for comparison with 0 mg BLM/ml (or a mean difference of 0 on the vertical axis). +, p<0.05 for comparison with no anti-ß1 integrin antibody. #, $p < 0.05$ for comparison with GFP siRNA-transfected cells.

Figure 6. Effect of BLM-induced on γH2AX immunofluorescence. MLEC were treated with 0-500 μg BLM/ml for 15 min, fixed and immunostained for γH2AX. (**A**) Representative fluorescence images with the concentration of BLM in μg/ml indicated in each frame. The bar in the upper left frame represents 40 μm. (**B**) Bars represent the mean nuclear fluorescence intensity + SE for 100-250 cells in each treatment group. *, p<0.05 comparison with 0 μg BLM/ml.

Figure 7. Effect of knockdown of Lig1, PARP-1, Lig3α and XRCC1 on β1 integrin engagement and BLM-induced γH2AX immunofluorescence. MLEC were transfected with 200 nM GFP (**A**), Lig1 (**B**), Lig3α (**C**), XRCC1 (**D**), and PARP-1 (**E**) siRNA. Twenty four h later ß1 integrins were engaged as in figure 3. Cells were then exposed to 0, 25 or 100 μg BLM /ml for 15 min and processed as in figure 5. Bars represent the mean nuclear fluorescence intensity + SE for 100-700 cells in each experimental group. *, p<0.05 comparison with 0 μg BLM/ml. +, p<0.05 comparison with no anti-ß1 integrin antibody.

Figure 8. Effect of knockdown of XRCC1 on integrin-mediated suppression of BLM-induced cytotoxicity. MLEC treated with medium (**A, B**) or 500 μg BLM/ml (**C, D**) for 4 h were photographed after 20 min incubation with ET2 and H33258 as described in the Methods. ET2 fluorescence (**A, C**) and H33342 fluorescence (**B, D**) in duplicate images are shown. The bar in the upper left frame represents 80 μm. MLEC were transfected with 200 nM GFP (**E**) or XRCC1 siRNA (**F**). Twenty four h later ß1 integrins were engaged as in figure 3. Cells were then treated with 0, 100 or 500 μg BLM/ml for 4 h, then incubated with ET2 and H33258 for 20 min, and

photographed. Bars represent the mean difference in nuclear ET2 fluorescence intensity between BLM- and vehicle-treated cells + SE for 350-1000 cells in each experimental group. *, p <0.05 for comparison with 0 µg BLM/ml (or a mean difference of 0 on the vertical axis). +, p<0.05 for comparison with no anti-ß1 integrin antibody. #, p <0.05 for comparison with GFP siRNA-transfected cells.
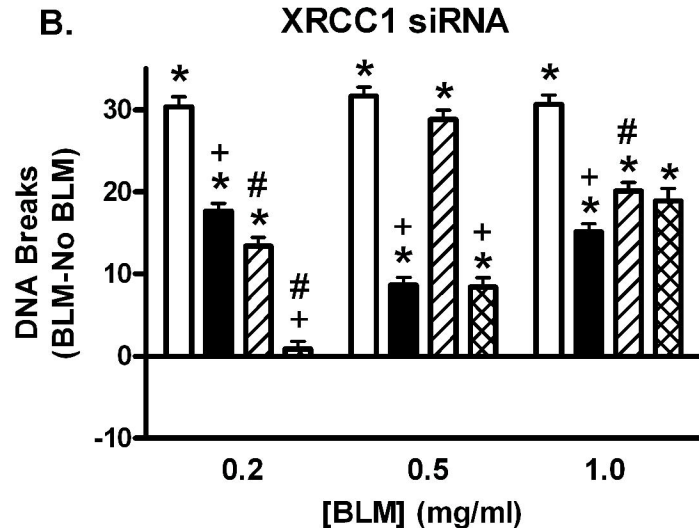
Figure 1.
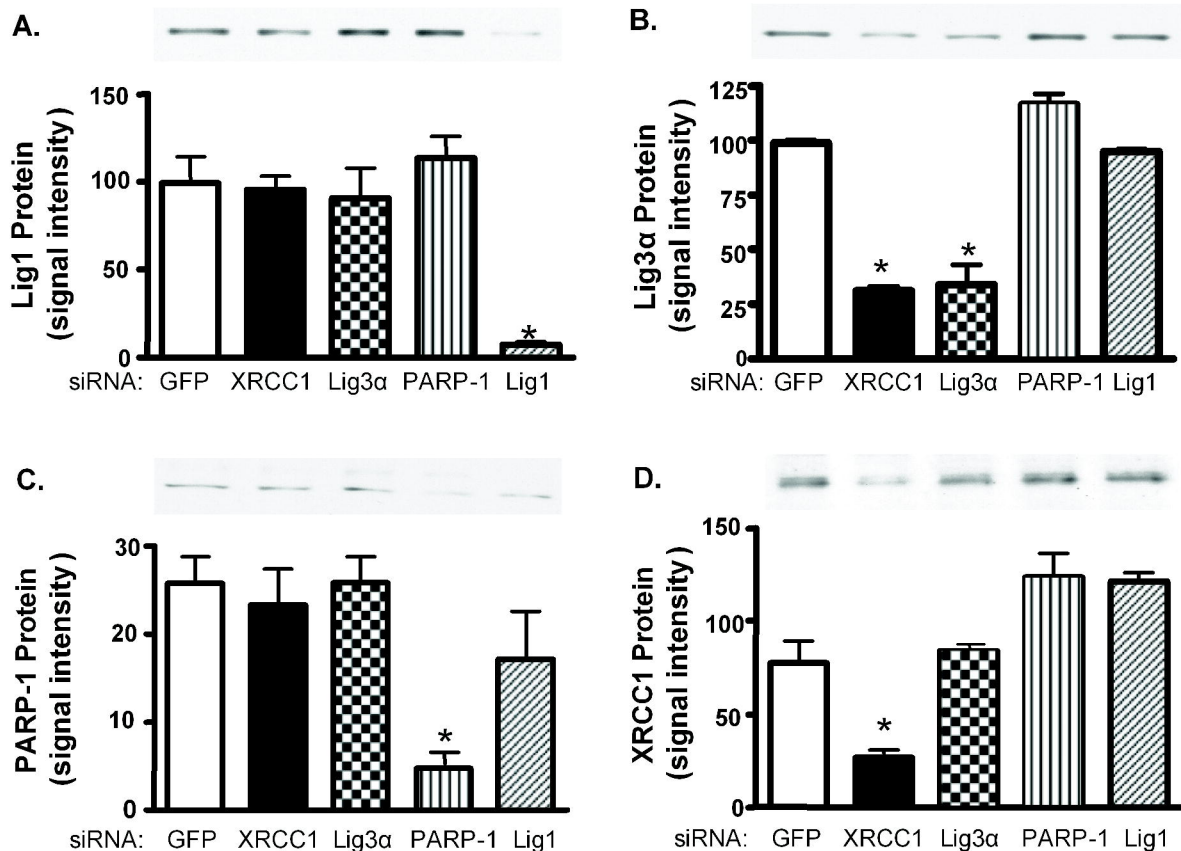
Figure 2.

Figure 3.
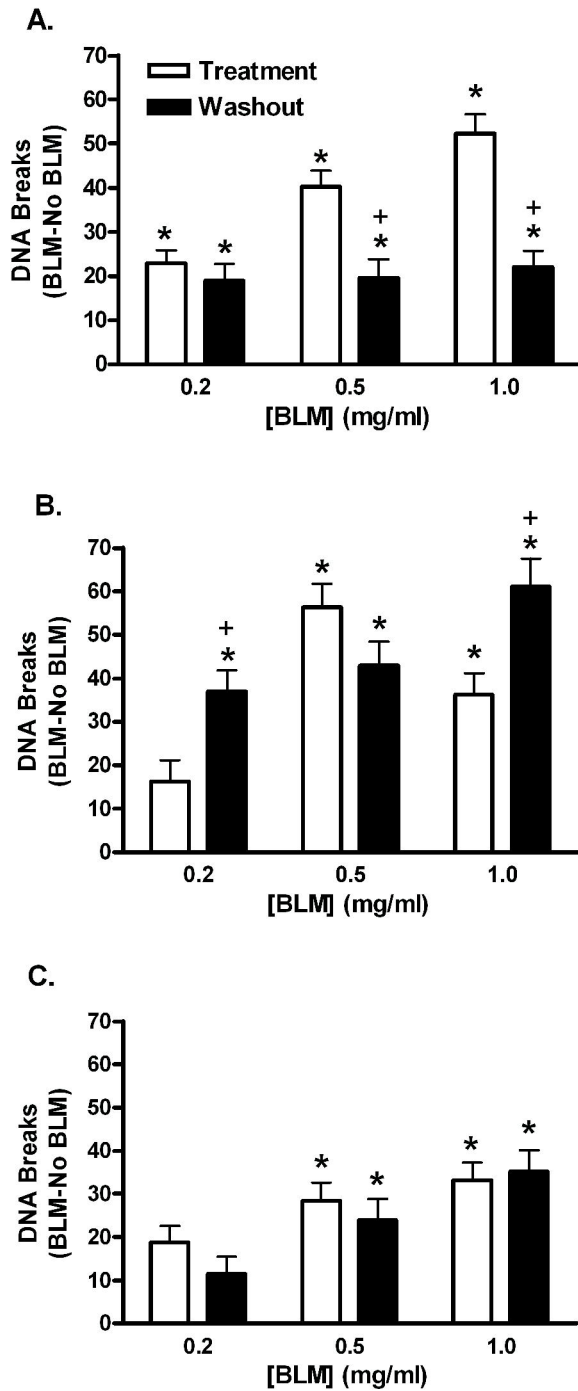
Figure 4.
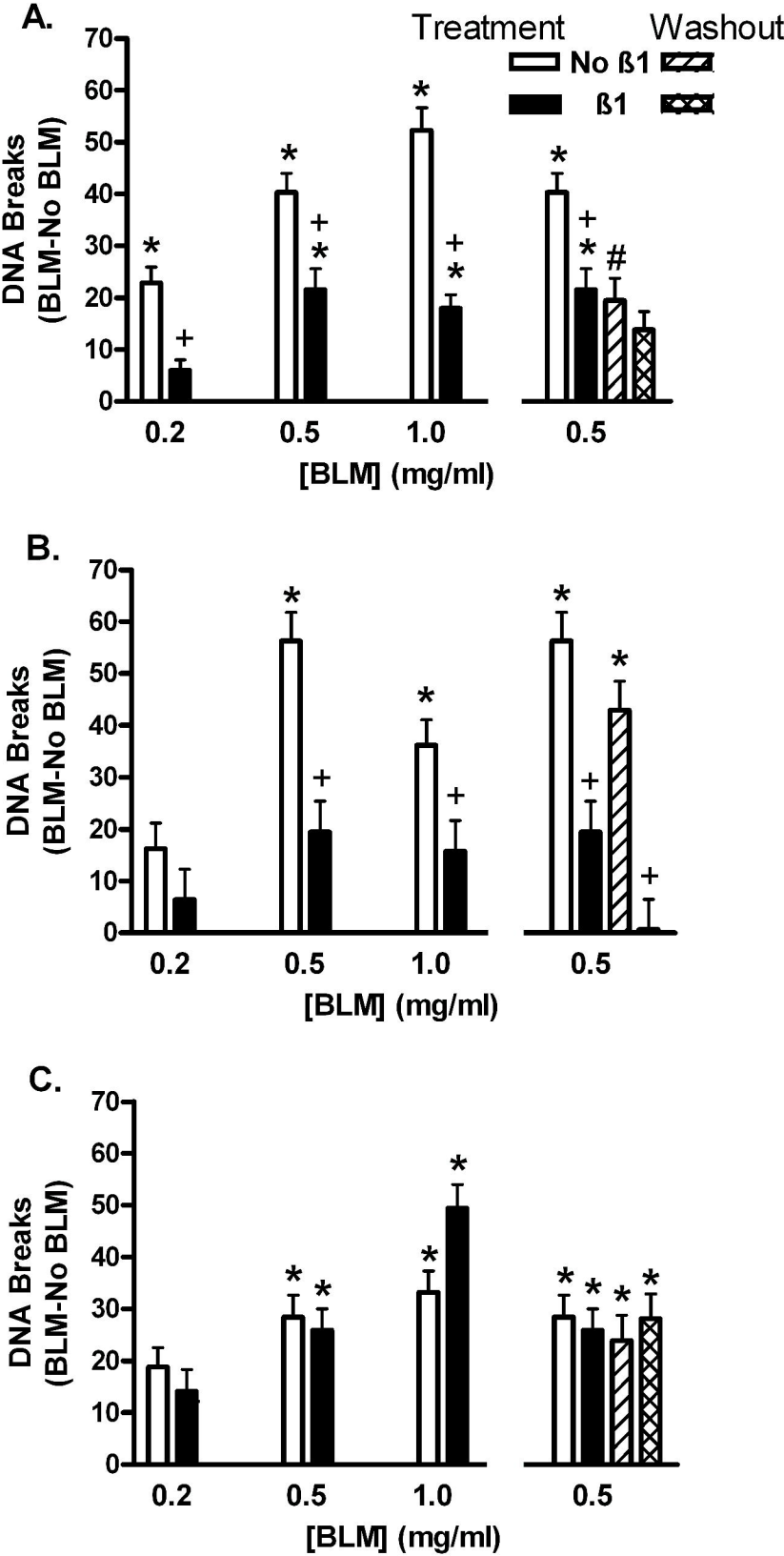
A. GFP siRNA
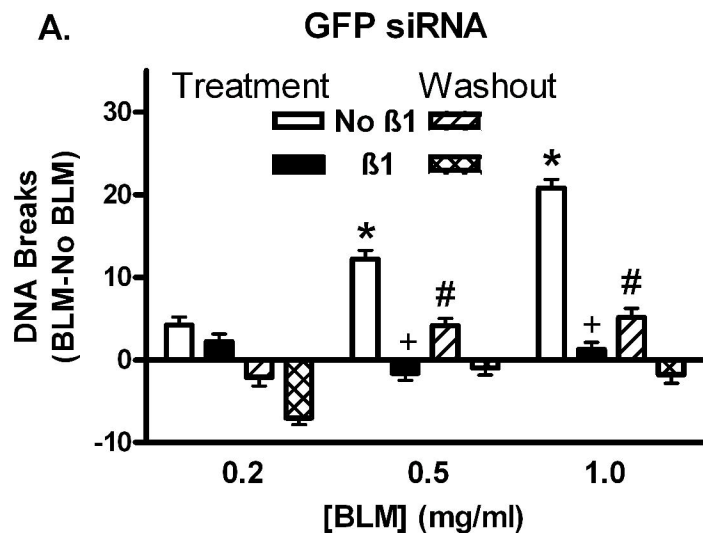
B. XRCC1 siRNA
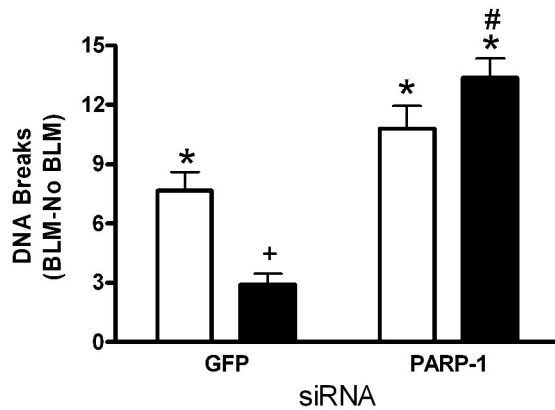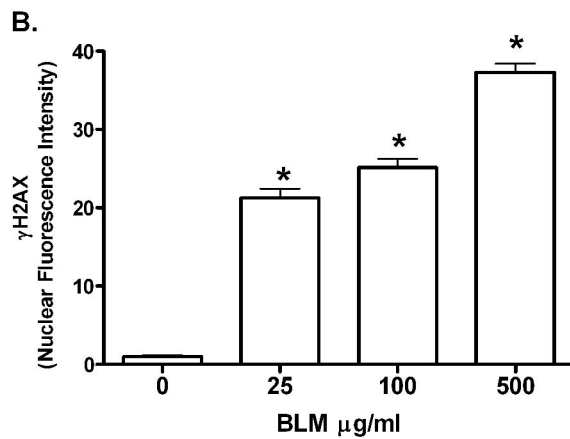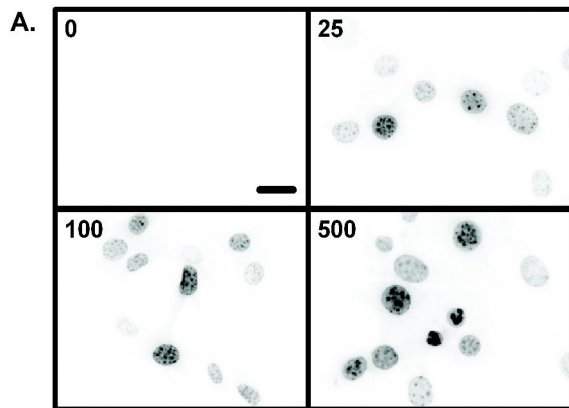
Figure 5.

Figure 6.

Figure 7.

A. GFP siRNA
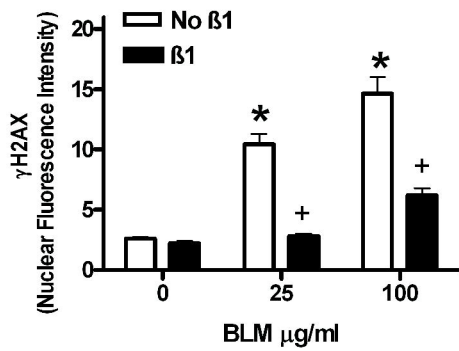
B. Lig1 siRNA
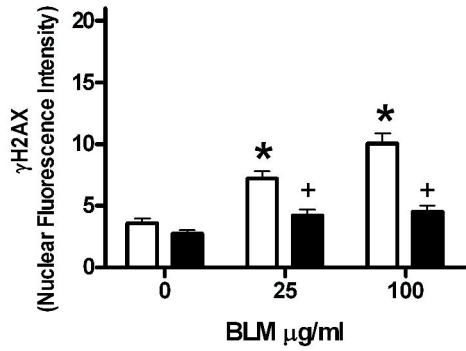
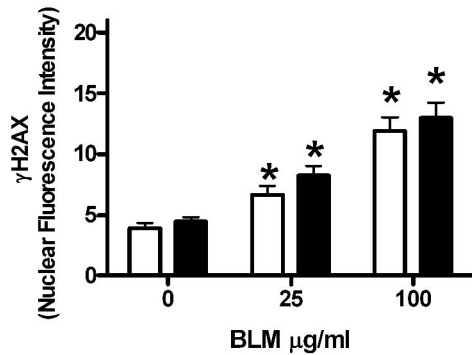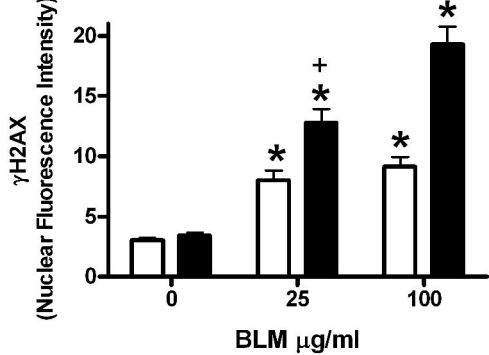## C. Lig3α siRNA

D. XRCC1 siRNA

E. PARP-1 siRNA

Figure 8.